E14-2012-31

T. Kalabegishvili[1,2], E. Kirkesali[1], A. Rcheulishvili[1], E. Ginturi[1], I. Murusidze[2], N. Kuchava[1], N. Bagdavadze[1], G. Tsertsvadze[3], V. Gabunia[4], M. V. Frontasyeva, S. S. Pavlov, I. Zinicovscaia, M. J. Raven[5], M. M. F. Seaga[5], A. Faanhof[6]

SYNTHESIS OF GOLD NANOPARTICLES BY BLUE-GREEN ALGAE *Spirulina platensis*

Submitted to «Journal of Applied Microbiology and Biotechnology»

[1]I. Javakhishvili State University, E. Andronikashvili Institute of Physics, Tbilisi, Georgia
[2]Ilia State University, Tbilisi, Georgia
[3]Georgian Technical University, Tbilisi, Georgia
[4]I. Javakhishvili State University, P. Melikishvili Institute of Physical and Organic Chemistry, Tbilisi, Georgia
[5]Nuclear Energy Corporation of South Africa (NECSA), Pelindaba, Pretoria, South Africa
[6]Centre of Applied Radiation Science & Technology, North-West University (Mafikeng Campus), Mafikeng, South Africa

Калабегишвили Т. и др. E14-2012-31

Синтез наночастиц золота сине-зеленой микроводорослью *Spirulina platensis*

Изучался синтез наночастиц золота одним из наиболее популярных микроорганизмов — сине-зеленой микроводорослью *Spirulina platensis*. Комплекс оптических и аналитических методов использовался для исследования образцов после их взаимодействия с раствором хлороаурата ($HAuCl_4$) в различных концентрациях и различных интервалах времени. Для характеристики полученных наночастиц золота применяли ультрафиолетовую спектрометрию, сканирующую и трансмиссионную электронную микроскопию, энергодисперсионный рентгеновский анализ и рентгеновскую дифрактометрию. Показано, что через 1,5–2 дня взаимодействия с раствором хлороаурата в образцах спирулины наблюдается внеклеточное образование наночастиц сферической формы со средними размерами 20–30 нм. Для определения концентрации золота в биомассе *Spirulina platensis* использовали нейтронный активационный анализ (НАА) и атомно-адсорбционную спектрометрию (ААС). Результаты указывают на быстрое увеличение концентрации золота в начале воздействия при незначительном увеличении в течение следующих нескольких дней. Полученная биомасса *Spirulina platensis* с наночастицами золота может быть использована для медицинских, фармацевтических и технологических целей.

Работа выполнена в Лаборатории нейтронной физики им. И. М. Франка ОИЯИ, Институте физики им. Э. Л. Андроникашвили АН Грузии и Южноафриканской корпорации по атомной энергии, Претория, ЮАР.

Препринт Объединенного института ядерных исследований. Дубна, 2012

Kalabegishvili T. et al. E14-2012-31

Synthesis of Gold Nanoparticles by Blue-Green Algae *Spirulina platensis*

The synthesis of gold nanoparticles by one of the many popular microorganisms — blue-green algae *Spirulina platensis* was studied. The complex of optical and analytical methods was applied for investigation of experimental samples after exposure to chloroaurate ($HAuCl_4$) solution at different doses and for different time intervals. To characterize formed gold nanoparticles UV-vis, TEM, SEM, EDAX, and XRD were used. It was shown that after 1.5–2 days of exposure the extracellular formation of nanoparticles of spherical form and the distribution peak within the interval of 20–30 nm took place. To determine gold concentrations in the *Spirulina platensis* biomass, neutron activation analysis (NAA) and atomic absorption spectrometry (AAS) were applied. The results obtained evidence that the concentration of gold accumulated by *Spirulina* biomass is rapidly growing in the beginning, followed by some increase for the next few days. The obtained substance of *Spirulina* biomass with gold nanoparticles may be used for medical, pharmaceutical, and technological purposes.

The investigation has been performed at the Frank Laboratory of Neutron Physics, JINR, at the E. L. Andronikashvili Institute of Physics of the Georgian Academy of Sciences, Tbilisi, and in the South African Nuclear Energy Corporation (NECSA), Pretoria, South Africa.

Preprint of the Joint Institute for Nuclear Research. Dubna, 2012

INTRODUCTION

Biosynthesis of nanoparticles using microorganisms as an emerging bionanotechnology has received considerable attention due to a growing need to develop environment-friendly technologies in materials synthesis [1]. Biological production systems are of special interest due to their effectiveness and flexibility. Nanoparticles produced by a biogenic enzymatic process are far superior in biomedical applications to those produced by chemical methods [2, 3].

Nanoparticles are biosynthesized when the microorganisms grab metal ions from environment and then turn them into nanoscale particles of elemental metal through enzymes generated by cell activities intracellularly or extracellularly [4]. The particles produced by these processes have higher catalytic reactivity, greater specific surface area, and an improved contact between the enzyme and metal salt in question due to the bacterial carrier matrix. They have been used in a variety of applications including drug carriers for targeted delivery, cancer treatment, gene therapy and DNA analysis, antibacterial agents, biosensors, enhancing reaction rates, separation science.

Gold nanoparticles play their significant role in nanotechnology due to their potential utilization in industry and medicine [5]. The gold nanoparticles were already used for curing various diseases centuries ago. Michael Faraday was the first to report that colloidal gold solutions had properties different from bulk gold [6]. In many investigations, the different microorganisms were used for producing nanoparticles. Sastry et al. have studied the extracellular synthesis of gold nanoparticles by fungi *Fusarium oxysporum* and *Verticillium* sp. and actinomycete *Thermomonospora* sp. [7–9]. Southam and Beverige have demonstrated that nanoparticles may readily be precipitated within bacterial cells by incubation at presence of Au ions [10, 11].

Monodisperse gold nanoparticles have been synthesized using alkalotolerant *Rhodococcus* sp. under extreme biological conditions [12]. Lengke et al. studied the synthesis of gold nanostructures of different shapes (spherical, cubic, and octahedral) by filamentous cyanobacteria and analyzed their formation mechanisms [13, 14]. Kumar et al. have observed the extracellular biosynthesis of silver, gold and bimetallic nanoparticles using *Spirulina platensis* (*S. platensis*) [15]. Govindaraju et al. studied synthesis of nanoparticles of Ag and Au by *S. platensis* because of its nutrient and pharmaceutical importance [16].

Spirulina is a filamentous plankton cyanobacterium, or a multicellular helical filamentous alga. It is one of the most concentrated natural sources of nutrition known in the world. This microalga is 60–70% vegetable protein, well balanced in amino acids, rich in beta carotene and iron, and the world's richest natural source of vitamins and essential fatty acids and other biologically active beneficial substances [17–19].

Blue-green microalgae *S. platensis* is widely used as a matrix for pharmaceuticals and also as a biologically active food additive for humans and animals. The ability to biotransform and endogenously add the desired essential elements (Se, I, Cr, and others) producing complexes easily assimilated by a human organism is a distinctive feature of *S. platensis*. Being a living organism, it accumulates elements strictly as much as is necessary for the organism.

In our earlier investigations *S. platensis* was used as a matrix for development of new pharmaceutical substances [20–23], as well as a biosorbent for remediation of waste waters [24]. The synthesis of silver nanoparticles by biomass of *S. platensis*, as well as by actinomycete *Streptomyces glaucus*, was studied in [25] and the synthesis of gold nanoparticles by *Arthrobacter* genera in [26]. In the present work the results of studies of Au nanoparticles synthesis by biomass of blue-green algae *S. platensis* are reported. A complex of spectral and analytical methods was used to characterize the experimental samples: UV-vis spectrometry, X-ray diffraction (XRD), transmission electron microscopy (TEM), scanning electron microscopy (SEM) with energy-dispersive analysis of X-rays (EDAX), neutron activation analysis (NAA), and atomic absorption spectrometry (AAS).

EXPERIMENTAL

Sample Preparation. In the experiments, the strain of *S. platensis* IPPAS B-256 from A. K. Timiriazev Institute for Plant Physiology of the Russian Academy of Sciences was used. The conditions of cultivation of *S. platensis* cells in standard Zaroukh water-salt nutrient medium are described elsewhere [21, 23]. All chemicals used in the experiment were ACS-reagent grade, produced by Sigma (St. Louis, MO, USA).

The bacterial cells were harvested after 5-6 days cultivation and then were washed twice in distilled water. In the first series of experiments, the dose dependency of the gold nanoparticles formation was studied. The wet biomass of *S. platensis* (1 g) was resuspended in 250 ml Erlenmeyer flasks with 100 ml aqueous $HAuCl_4$ (chloroaurate) solution with different concentrations (10^{-2}–10^{-4}M) and incubated at the room temperature for 5 days being shaken continuously.

In the second series of experiments, the temporal dependency of Au nanoparticles formation was studied. Again 1 g of wet biomass was resuspended in the

same flasks with 100 ml 10^{-3}M aqueous $HAuCl_4$ solution and incubated at room temperature, shaking for different time intervals (1–6 days).

For UV-vis spectral analysis and TEM, 5 ml samples of the suspension were taken in the first experiment after 5 days and in the second experiment — after different time intervals. For SEM, X-ray, AAS, and NAA, the bacterial cells in each case were harvested by centrifugation at 12 000 g for 20 min. The wet biomass was placed in an adsorption-condensation lyophilizer [27] and dried until constant weight.

Methods. *UV-VIS Spectrometry.* The UV-visual spectra of the samples were recorded by a spectrophotometer «Cintra 10» (GBC Scientific Equipment Pty Ltd, Australia) with digital data acquisition system, wavelength range 190–1100 nm.

X-Ray Diffraction (XRD). XRD measurements of the *S. platensis* biomass were performed at a Dron-2.0 diffractometer. The BCV-23 X-ray tube with the Cu anode (CuK_α: $\lambda = 1.54178$ Å) was used as a source of radiation; the Ni grid with a width of 20 μm was used for filtration of the radiation; the rate of the detector was 2°/min, the interval of intensity was 1000 pulses/min and the time constant was 5 s.

Transmission Electron Microscopy (TEM). TEM was performed using the JEOL SX-100 equipment (Japan) operating at 100 kV. The TEM studies were done at 50 000 x magnification. Samples were prepared by placing a drop of solution with the gold nanoparticles on carbon-coated TEM grids. The films on the TEM grids were allowed to dry at room temperature before analysis.

Scanning Electron Microscopy (SEM). The FEI Quanta 3D FEG, USA / Systems for Microscopy and Analysis, (Moscow, Russia) high-performance instrument with three modes was used for sample visualization.

SEM was carried out using the SDB (small dual-beam) FEI Quanta 3D FEG with the EDAX Genesis system with the resolution 1.2 nm. Operational features of the microscope used in the experiment: magnification 5000–150 000 x; voltage 1–30 kV.

Energy-Dispersive Analysis of X-Rays (EDAX). To identify different elements associated with the studied sample specimen, the «built-in» Energy Dispersive X-ray Analysis (EDAX) spectrometer was used. EDAX is an analytical technique which utilizes X-rays that are emitted from a specimen when bombarded by an electron beam to identify the elemental composition of a specimen. The EDAX X-ray detector measures the number of emitted X-rays versus their energy [20].

Microprobe analysis of gold nanoparticles clusters was conducted with the energy-dispersive X-ray analysis spectrometer (EDAX, USA). The acquisition time ranged from 60 to 100 s, and the accelerating voltage was 20 kV.

Atomic Absorption Spectrometry (AAS). A flame AAS with a «Beckman-495» spectrometer was used for gold determination in the experimental samples. Measurement was carried out at the wavelength of the gold resonance line $\lambda = 242.8$ nm.

Neutron Activation Analysis (NAA). The gold concentration in *S. platensis* samples was determined by neutron activation analysis (NAA) at the nuclear research reactor SAFARI-1 of the NECSA (Nuclear Energy Corporation of South Africa), Pelindaba, South Africa. The samples were irradiated for 8 s by a neutron flux density of approximately 10^{14} n $\cdot$ cm$^{-2} \cdot$ s^{-1}. Their activities were measured three times, after cooling for 3 and 30 hours and after 7 days, respectively. The gold content was determined on the 411.8 keV γ-line of ^{198}Au.

The elemental content of *S. platensis* samples was determined using NAA at the reactor IBR-2 of FLNP, JINR, Dubna, Russia. The concentrations of elements based on short half-life radionuclides were determined by irradiation for 60 s under a thermal neutron flux density of approximately $1.6 \cdot 10^{13}$n $\cdot$ cm$^{-2} \cdot$ s^{-1}. The NAA data processing and determination of element concentrations were performed using genie 2000 software, results and discussion.

RESULTS AND DISCUSSION

The UV-vis absorption spectra of the suspension of *S. platensis* after addition of the chloroaurate solution in different concentrations (the dose dependence) are shown in Fig. 1, *a*. As seen from the figure, one broad peak of gold surface plasmon resonance (SPR) appears at 530 nm for the concentrations of 10^{-3}–10^{-4} M. The presence of the gold (SPR) peak at $\sim$ 530 nm confirms the gold ion reduction from Au(III) to Au(0) by biomolecules/proteins and enzymes on the surface of *S. platensis* cells and aggregation of the gold nanoparticles in the solution.

At higher concentrations of $HAuCl_4$(10^{-2}M) such a peak was not observed. In the work [28], it is hypothesized that the number of active objects on the surface of *S. platensis* cells involved in the synthesis is not sufficient for reduction of gold ions at higher concentrations. Consequently, the synthesis process depends

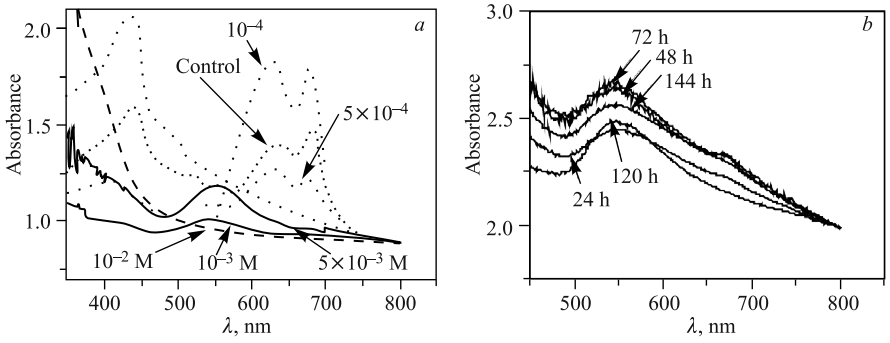

Fig. 1. UV-vis spectra of *S. platensis* suspension for different doses of chloroaurate (*a*) and for different time exposure (*b*)

on the gold concentration as well as on the number of cells in solution. This differential response indicates the possibility of production of custom-designed nanoparticles by varying cell number and gold concentration in solution.

Thus, for the second series of experiments, the solution of chloroaurate in concentration 10^{-3} M was used. The UV-vis spectra of *S. platensis* suspension for the different time of the cell cultivation in presence of Au compound (the temporal dependence) are shown in Fig. 1, *b*. The intensity of the peak increases as a function of the reaction time. As is known, the position of the plasmon adsorption peak of gold nanoclusters strongly depends on the particles size, dielectric constant of the medium and the surface-adsorbed species. According to Mie's theory, only a single SPR band is expected in the adsorption spectra of spherical nanoparticles, whereas anisotropic particles could give rise to two or more SPR bands depending on the shape of the particles [29]. In the present case a single band was observed that gives evidence for the presence of spherical shape gold nanoparticles that was confirmed by TEM and SEM images.

Figure 2 shows the TEM image recorded from the drop-cast film of gold nanoparticles synthesized after reaction of the chloroauric acid $5 \cdot 10^{-3}$ M solution

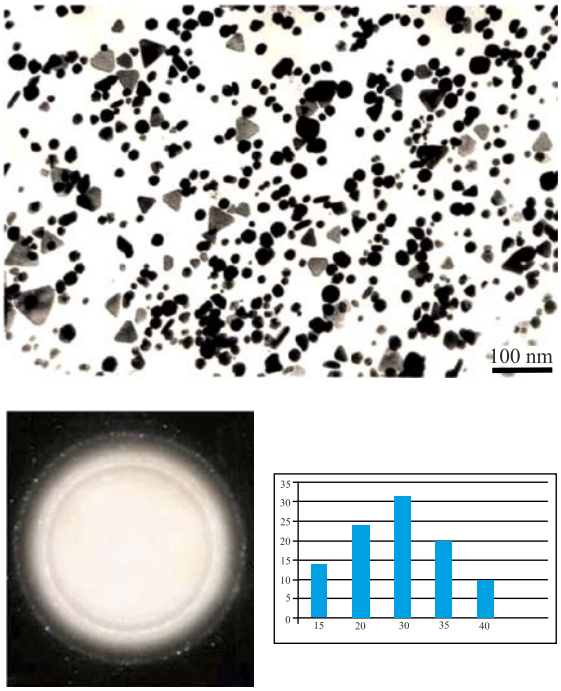

Fig. 2. TEM image, selected area diffraction pattern and size histogram of Au nanoparticles in biomass of *S. platensis*

with *S. platensis* biomass for 5 days. In the picture, the nanoparticles of spherical and other shapes are observed. Here the patterns correspond to the face centered cubic (fcc) structure of gold nanoparticles. The particle size histogram shows that the size of the gold nanoparticles ranges from 15 nm to 60 nm, and the majority of them have the size of about 30 nm.

The X-ray diffraction method was used for investigation of three samples of *S. platensis* biomass with the gold nanoparticles formed in a solution of $HAuCl_4$ at the concentrations 10^{-3}, $5 \cdot 10^{-3}$ and 10^{-2} M. In all cases, the diffractograms showed the presence of gold crystals of cubic form with the lattice parameter 4.077 Å characteristic of Au.

In Fig. 3, an XRD pattern of gold nanoparticles synthesized by treating *S. platensis* with chloroauric acid aqueous 10^{-3} M solution for 4 days is presented as an example. A number of Bragg's reflections corresponding to the fcc structure of gold are seen here: four characteristic peaks (111), (200), (220), and (311). The obtained results clearly show that gold nanoparticles formed by reduction of Au(III) ions by *S. platensis*, are crystalline in nature and they are generally produced extracellularly.

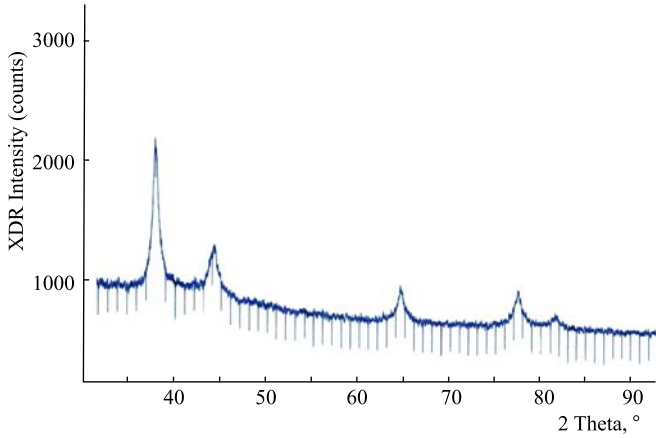

Fig. 3. XRD spectrum of Au nanoparticles in biomass of *S. platensis*

The Scherrer equation was used for an approximate estimation of the size of nanoparticles using the size of maximum intensity on the diffractogram:

$$d = K\lambda/\beta \cos\theta,$$

where K is the shape factor; for cubic crystals it is 0.9–1; λ is the X-ray wavelength, for CuK_α; $\lambda = 1.54178$ Å; β is the line broadening at half the maximum intensity in radians; θ is the Bragg angle, and d is the size of a

nanoparticle in nm. It is important to realize that the Scherrer formula is applicable to grains less than 0.1 μm in size [30, 31].

For the approximate evaluation of the size of nanoparticles (111) interferential maximum was used. In this case $\beta = 38°$. The calculations were carried out taking into account only apparatus uncertainty of $\beta\,(\approx 0.3°)$ without evaluation of the other defects on the maximums shape. The results obtained show that at the concentration of $HAuCl_4$ 10^{-3} M the size of gold nanoparticles is ≈ 14 nm, at $5 \cdot 10^{-3}$M — ≈ 20 nm, and at 10^{-2} M — ≈ 100 nm.

Figure 4 presents the SEM image of *S. platensis* cells after interacting with chloroaurat solution at different concentrations: $5 \cdot 10^{-3}$ M and 10^{-2} M for 5 days. The mode of the natural environment (ESEM) allows studying moist and nonconducting samples. Since *Spirulina* cells are nonconducting, they were visualized at this mode. The SEM images for concentration $5 \cdot 10^{-3}$ M illustrate that most of the particles are spherical and do not create big agglomerates whereas at concentration 10^{-2} M the size of formed particles is not in a nanoscale range.

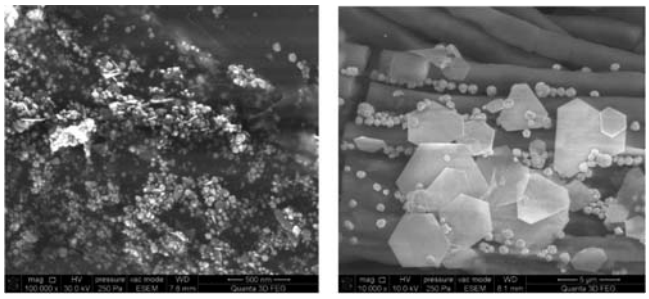

Fig. 4. SEM pictures of gold nanoparticles in *S. platensis* under the different chloroauric acid concentrations: $5 \cdot 10^{-3}$ M (left) and 10^{-2} M (right)

In Fig. 5, the SEM images of biomass of *S. platensis* after interacting with $HAuCl_4$ $5 \cdot 10^{-3}$ M for 24 hours and 5 days are shown. The comparison of these two images revealed the great number of gold nanoparticles formed by the biomass of *S. platensis* extracellularly after 6 days.

The EDAX X-ray spectra proved the presence of gold nanoparticles in *S. platensis* cells treated with 10^{-3}M solution of $HAuCl_4$ (Fig. 6). The energy of X-rays is characteristic of the elements from which these X-rays are emitted. A spectrum of the energy *versus* relative counts of the detected X-rays is presented in Fig. 6. Three peaks of Au were observed for biomass of *S. platensis*. The signals from C, O, and Cl atoms were also recorded. These signals are likely to be due to X-ray emission from the proteins and enzymes present in the cell wall of the biomass.

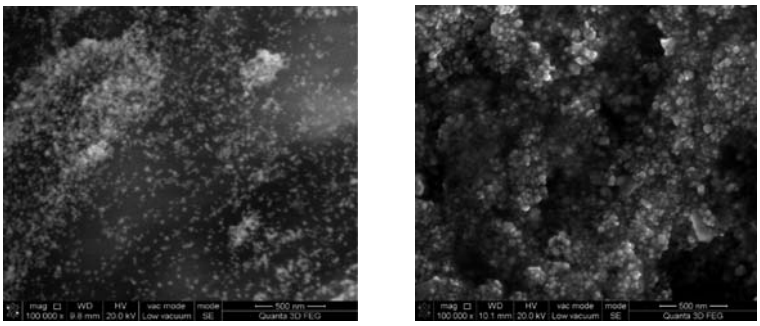

Fig. 5. SEM pictures of gold nanoparticles in *S. platensis* at different incubation time: 24 hours (left) and 5 days (right)

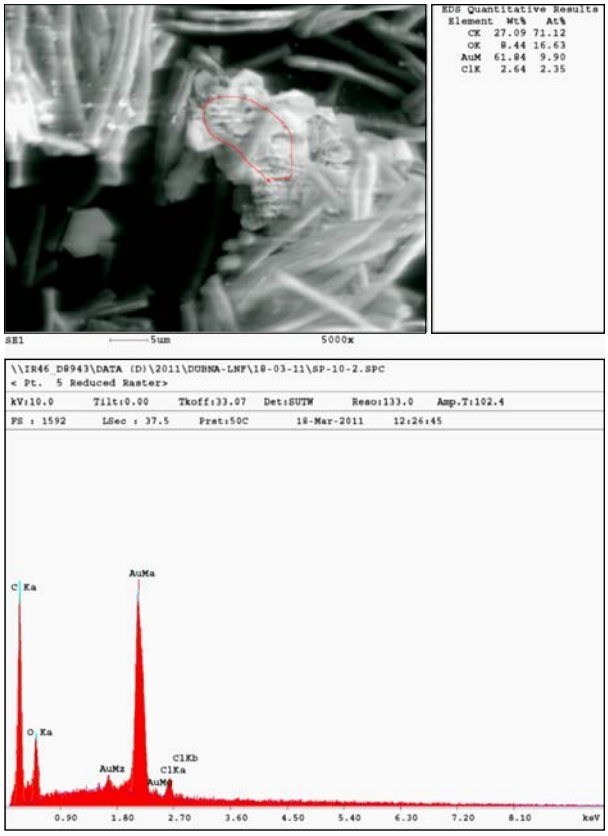

Fig. 6. EDAX spectrum of *S. platensis* biomass with the gold nanoparticles

The data of the total concentrations of gold in *S. platensis* biomass and supernatant obtained by AAS for different dose (*a*) and different time of chloroaurate exposure (*b*) are presented in Fig. 7. The increase of the gold concentrations in biomass of *S. platensis* leads to its decrease in supernatant. The time dependence illustrates that uptake of gold includes two phases: rapid and slower. In the first «rapid» stage, the metal ions are adsorbed onto the surface of microorganism. The concentration of gold increases rapidly (within few minutes).

The cell wall of *S. platensis* contains functional groups within biomolecules (amino, carboxylic, phosphate, thiol and other) that can bind metal ions. In the «slow» stage (a few days), the metal ions are transported across the cell membrane into the cytoplasm.

The results of NAA for Au obtained at the nuclear research reactor SAFARI-1 are presented in Fig. 8, *a, b*. The total concentrations of gold in *S. platensis* biomass for different doses of chloroaurate presented in Fig. 8, *a, b* show that the total concentration of gold in samples (extracellular and intracellular) is rapidly increasing in the beginning and then does not change over time

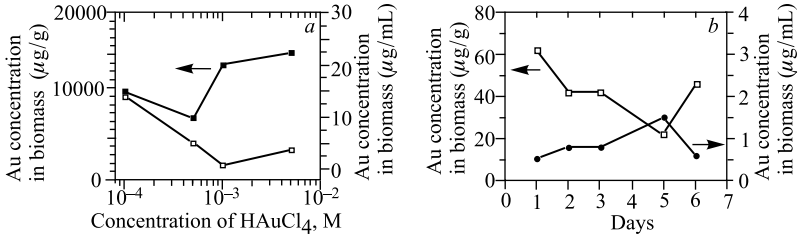

Fig. 7. The gold concentrations in biomass of *S. platensis* and in supernatant *versus* the concentration of chloroauric acid (*a*) and the time of exposure to chloroauric acid (*b*) determined by AAS

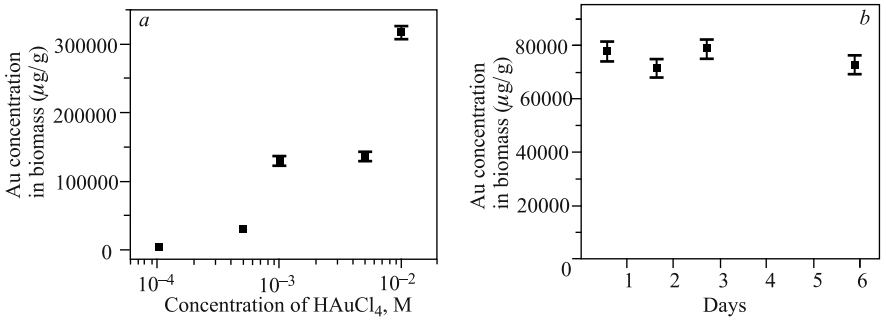

Fig. 8. The gold concentrations in biomass of *S. platensis versus* the concentration of chloroauric acid (*a*) and the time of exposure to chloroauric acid (*b*) determined by NAA

significantly. The other elements in the given experiment in the presence of high Au concentrations were not determined.

The concentrations of the matrix elements Mg, Mn, Cl, Ca, P and the traces of U in the biomass of *S. platensis* were determined at the reactor IBR-2 based on short half-life radionuclides.

CONCLUSIONS

The results of the presented studies using the complex of optical and analytical methods show that *S. platensis* is capable of producing gold nanoparticles extracellularly when exposed to the gold chloroaurate solution. The shape of the majority of the nanoparticles is spherical and on average their sizes are in the range 20–30 nm. The «green route» of biosynthesis of gold nanoparticles in *Spirulina* is simple, economically viable and an eco-friendly process which offers a great advantage over an intracellular process of synthesis from the point of view of applications in medicine, pharmacology and other branches of technology.

Acknowledgements. This work was financially supported by the Ukrainian Science and Technology Centre (STCU Grant No. 4744) and Grant of JINR-South Africa (Order No. 69, 2012).

REFERENCES

1. *Rai M., Gade A., Yadav A.* Biogenic Nanoparticles: An Introduction to What They Are, How Are Synthesized and Their Applications / Ed.: Rai M. Duran N. // Metal Nanoparticles in Microbiology, Berlin, Springer-Verlag GmbH, 2011. P. 1–14.
2. *Li X. et al.* // J. Nanomater. 2011. doi:10.1155/2011/270974.
3. *Mandal D. et al.* // Appl. Microbiol. Biotechnol. 2006. V. 69. P. 485–492.
4. *Lengke M. F., Sanpawanitchakit C., Southan G.* // Metal Nanoparticles in Microbiology / Ed.: Rai M., Duran N. Berlin, Springer-Verlag GmbH. 2011. P. 37–74.
5. *Sadowski Z.* Wroclaw University of Technology, 2009. P. 257–276.
6. *Hayat M. A.* Colloidal Gold: Principles, Methods, and Applications, San Diego, Academic Press, 1989.
7. *Mukherjee P. et al.* // Chem. Biochem. 2002. V. 3. P. 461–463.
8. *Ahmad A. et al.* // Langmuir. 2003. V. 19. P. 3550–3553.
9. *Mukherjee P. et al.* // Angew. Chem. Int. 2001. V. 40. P. 3585–3588.
10. *Southam G. et al.* // Geochim. Cosmochim. Acta. 1996. V. 60. P. 4369–4376.
11. *Southam G. et al.* // Geochim. Cosmochim. Acta. 1994. V. 58. P. 4527–4530.
12. *Ahmad A. et al.* // Nanotechnology. 2003. V. 14. P. 824–828.
13. *Lengke M. F. et al.* // Environ. Sci. Technol. 2006. V. 20. P. 6304–6309.
14. *Lengke M. F. et al.* // Langmuir. 2006. V. 22. P. 2780–2787.

15. *Kumar V. G. et al.* // J. Mater. Sci. 2006. V. 43. P. 5115–5122.
16. *Govindaraju K. et al.* // J. Mater Sci. 2008. V. 43. P. 1164–1170.
17. *Ciferri O.* // Microbiol. Rev. 1983. V. 47. P. 551–578.
18. *Belay A. et al.* // J. Appl. Phycol. 1993. V. 5. P. 235–241.
19. *Doshi H. et al.* // Biotechnol. Bioeng. 2007. V. 96. P. 1051–1063.
20. *Mosulishvili L. M. et al.* // J. Neutron. Res. 2007. V. 15. P. 49–54.
21. *Mosulishvili L. M. et al.* // J. Pharmaceut. Biomed. Anal. 2002. V. 30. P. 87–97.
22. *Mosulishvili L. M. et al.* Patent of RF No. 2230560, 2002.
23. *Mosulishvili L. M. et al.* Patent of RF No. 2209077, 2001.
24. *Frontasyeva M. V. et al.* // J. Neutron Res. 2006. V. 14. P. 131–137.
25. *Tsibakhashvili N. Y. et al.* // Adv. Sci. Lett. 2011. V. 4. P. 1–10.
26. *Kalabegishvili T. et al.* // J. Mater. Sci. Eng. 2012. V. 2. P. 164–173.
27. *Mosulishvili L. M. et al.* Patent URSS, No. 779765, 1980.
28. *Pimprikar P. S. et al.* // Colloids Surf. B. 2009. V. 74. P. 309–316.
29. *Sosa O. et al.* // J. Phys. Chem. B. 2003. V. 107. P. 6269–6275.
30. *Cullity B. D., Stock S. R.* Elements of X-Ray Diffraction. New Jersey, Prentice-Hall Inc, 2001.
31. *Jenkins R., Snyder R.L.* Introduction to X-Ray Powder Diffractometry. New York, John Wiley & Sons Inc, 1996.

Received on March 20, 2012.

Редактор *Э. В. Ивашкевич*

Подписано в печать 08.06.2012.
Формат 60 × 90/16. Бумага офсетная. Печать офсетная.
Усл. печ. л. 0,87. Уч.-изд. л. 1,28. Тираж 260 экз. Заказ № 57667.

Издательский отдел Объединенного института ядерных исследований
141980, г. Дубна, Московская обл., ул. Жолио-Кюри, 6.
E-mail: publish@jinr.ru
www.jinr.ru/publish/